The Control of Space Manipulators Subject to Spacecraft Attitude Control Saturation Limits

S. Dubowsky, E. E. Vance*, M. A. Torres**

Department of Mechanical Engineering
Massachusetts Institute of Technology
Cambridge, MA 02139

Abstract

The motions of robotic manipulators mounted on spacecraft can disturb the spacecraft's positions and attitude. These disturbances can surpass the ability of the system's attitude control reaction jets to control them, for the disturbances increase as manipulator speeds increase. If the manipulator moves too quickly the resulting disturbances can exceed the saturation levels of the reaction jets, causing excessive spacecraft motions. This paper presents a method for planning space manipulator,s motions so that tasks can be performed as quickly as possible without saturating the system's attitude control jets.

1. Introduction

This paper presents a method that enables space manipulator motions to be planned so that tasks can be performed in minimum time, without saturating the system's attitude control jets.

Future space missions are expected to use robotic manipulators mounted on spacecraft to construct space stations and repair satellites. However, the motions of such manipulators can disturb the position and attitude of their spacecraft. While control techniques have been proposed for space manipulators which permit their spacecraft to move in response to manipulator motions [1], for many missions even relatively small unplanned spacecraft motions may be undesirable. Although these motions can be controlled using the spacecraft's attitude control reaction jets, disturbances increase as manipulator speeds increase. Even with the use of recently developed methods for planning space manipulator motions to minimize the disturbances [2,3], these disturbances can exceed the saturation levels of the spacecraft reaction jet system and result in excessive spacecraft motions. Therefore, motion planning for space manipulators must consider the limits of the reaction jets if space manipulators are to be able to perform their tasks quickly, in minimum time, without excessive spacecraft motions.

A number of methods have been developed to plan the minimum time motion of *fixed based* manipulators [4-9]. However these methods do not consider the problem of the motion planning for *space manipulators* with their spacecraft control systems saturation constraints . The technique presented here considers the saturation limits of both a manipulator's joint actuators and those of the reaction jets. It can be applied to any rigid, non-redundant space manipulator system whose actuator and spacecraft capabilities can be specified as a function of the state of the system. It provides both the optimal position and velocity command profiles for the system and the optimal open-loop actuator

* Now at the Center for Naval Analyses, Alexandria, VA.

** NASA Fellow.

and reaction jet forces and torques required for a given task. These forces and torques can be used as feedforward signals by manipulator and spacecraft closedloop control systems to reduce dynamic control system errors. The technique can also be used with conventional planning methods to aide in planning nonoptimal manipulator motions that will not exceed the system's capabilities.

Results demonstrate the effectiveness of the method for planning minimum time space manipulator motions. They also show that the technique can be used to design the lightest weight system to perform a given set of tasks in a specified amount of time.

2. The System

The technique is illustrated by its application to a simple system consisting of a three degree-of-freedom (DOF) revolute manipulator mounted on a spacecraft with six DOF, see Figure 1. The system has a total of nine DOF. The spacecraft is equipped with six reaction jets which can counteract the disturbance forces and moments generated by the manipulator's motion.

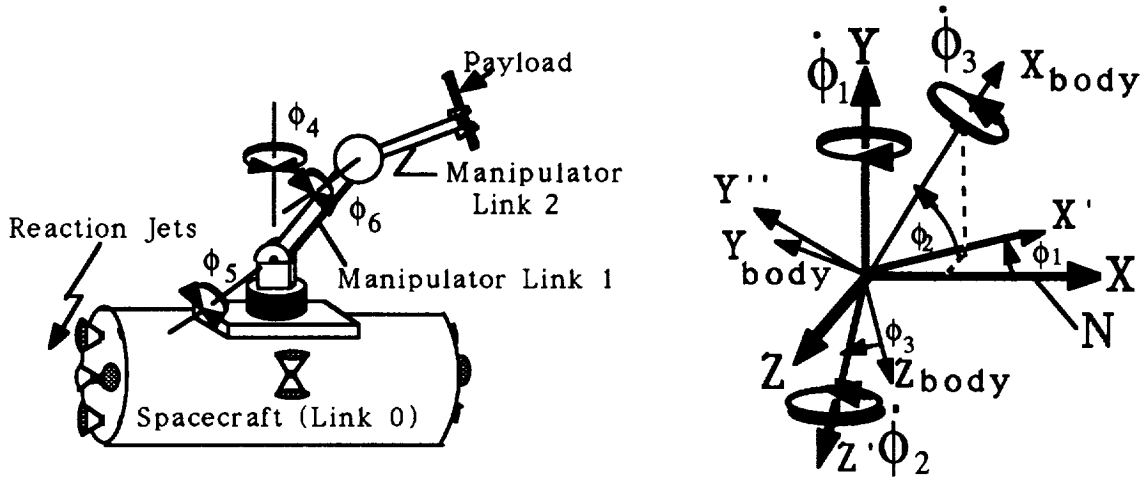

a. System and Manipulator Joint Variables. b. Spacecraft Rotation Variables.

Figure 1. System Model and Variables

The spacecraft's six DOF are represented by the variables X, Y, Z, ϕ_1, ϕ_2 and ϕ_3 which define its position and orientation with respect to the inertial coordinate frame **N**, also shown in Figure 1. A body-fixed coordinate frame (X_{body},Y_{body},Z_{body}) is attached to the spacecraft at its center of mass. The angle ϕ_1 is the rotation of the spacecraft about the Y_{body} axis, ϕ_2 is the rotation about the Z_{body} axis, and ϕ_3 is the rotation about the X_{body} axis, as shown in Figure 1b. The three manipulator joint motions, ϕ_4, ϕ_5 and ϕ_6, are shown in Figure 1a.

3. The Dynamic Model

The planning algorithm requires a full nonlinear dynamic model of the system. These equations may be formulated in any convenient manner. Here a Lagrangian formulation was used to develop the the dynamic equations for the system shown in Figure 1 with X, Y, Z, ϕ_1, ϕ_2, ϕ_3, ϕ_4, ϕ_5 and ϕ_6 as generalized coordinates. The resulting dynamic equations may be written in the vector form [10]:

$$\mathbf{M}_{\phi}\ddot{\underline{\phi}} + \dot{\underline{\phi}}\,\overset{<}{\mathbf{C}}_{\phi}\,\dot{\underline{\phi}} = \mathbf{T} \qquad (1)$$

where

$\underline{\phi}$ is a 9 element vector of generalized coordinates,
$\mathbf{M}_{\phi}$ is a 9x9 mass matrix,
$\overset{<}{\mathbf{C}}_{\phi}$ is a 9x9x9 Coriolis tensor, and
$\mathbf{T}$ is a 9 element vector of generalized forces and moments.

The elements of the Coriolis tensor, can be calculated from:

$$\overset{<}{\mathbf{C}}_{\phi ijk} = \frac{\partial \mathbf{M}_{\phi ij}}{\partial \phi_k} - \frac{1}{2}\frac{\partial \mathbf{M}_{\phi kj}}{\partial \phi_i} \qquad (2)$$

This nonlinear matrix equation was used in an independent dynamic simulation of the system to verify the results of the planning algorithm. When the objective of the optimization is to maintain a stationary spacecraft, a simplified form of Equation (1) can be used in the algorithm. It is obtained by setting the time derivatives of the spacecraft's generalized coordinates to zero. This simplification must be done after the complete equations of motion have been derived; setting these variables equal to zero before the Lagrangian differentiation leads to errors [10]. The resulting simplified equations have the form:

$$\begin{bmatrix} m_{17} & m_{18} & m_{19} \\ m_{27} & m_{28} & m_{29} \\ m_{37} & m_{38} & m_{39} \\ m_{47} & m_{48} & m_{49} \\ m_{57} & m_{58} & m_{59} \\ m_{67} & m_{68} & m_{69} \\ m_{77} & m_{78} & m_{79} \\ m_{78} & m_{88} & m_{89} \\ m_{79} & m_{89} & m_{99} \end{bmatrix} \begin{bmatrix} \ddot{\phi}_4 \\ \ddot{\phi}_5 \\ \ddot{\phi}_6 \end{bmatrix} + \begin{bmatrix} \dot{\phi}_4 \\ \dot{\phi}_5 \\ \dot{\phi}_6 \end{bmatrix}^T \begin{bmatrix} \begin{bmatrix} c_{77} & c_{78} & c_{79} \\ c_{78} & c_{88} & c_{89} \\ c_{79} & c_{89} & c_{99} \end{bmatrix}_1 \\ \vdots \\ \begin{bmatrix} c_{77} & c_{78} & c_{79} \\ c_{78} & c_{88} & c_{89} \\ c_{79} & c_{89} & c_{99} \end{bmatrix}_9 \end{bmatrix} \begin{bmatrix} \dot{\phi}_4 \\ \dot{\phi}_5 \\ \dot{\phi}_6 \end{bmatrix} = \begin{bmatrix} T_1 \\ T_2 \\ T_3 \\ T_4 \\ T_5 \\ T_6 \\ T_7 \\ T_8 \\ T_9 \end{bmatrix} \qquad (3)$$

where the elements of the simplified mass matrix and Coriolis tensor are subsets of the original full mass matrix and Coriolis tensor respectively.

4. The Planning Algorithm

The minimum time planning technique presented here is based on a well known algorithm developed for optimizing the motions of conventional manipulators along fixed paths [5], which has also been extended to non-fixed manipulator paths [6]. This algorithm is based on the fact that the minimum time motion of a manipulator along its path is achieved when its acceleration or deceleration is at its maximum at every point along the path. The algorithm finds the switching points between

the maximum acceleration and deceleration regions of the path using a function called the Limit Curve.

The Limit Curve, $\dot{S}_m(S)$, is generally plotted in the S - $\dot{S}$ phase plane and is the plot of the maximum velocity that the manipulator may have at any distance S along the path without exceeding the system's capabilities. To find the Limit Curve for a space manipulator, including the constraints imposed by the system's reaction jets Equations (1) must be transformed from an equation in terms of n generalized coordinates to an equation in terms of a scalar path coordinate, such as S, the distance along the path [5]. For a non-redundant space manipulator, the prescribed motion of the manipulator and the spacecraft may be written as a vector function of the generalized coordinates in the form:

$$\mathbf{P}(S) = \mathbf{R}(\phi) \tag{4}$$

where $\mathbf{P}$ is generally a 12 element vector representing the position and orientation of the manipulator end-effector and spacecraft, generally given in inertial coordinates. Only a three element $\underline{P}$ vector is required for the system shown in Figure 1 because the motion of the base is nominally stationary and the manipulator has only three DOF. Using Equation (4) and its derivatives, it is possible to transform the equations of motion, Equation (1), into an equation of the form [10]:

$$\underline{m}(\phi)\,\ddot{S} + \underline{b}(\phi)\,\dot{S}^2 = \mathbf{T} \tag{5}$$

The elements of the $\mathbf{T}$ vector in Equation (5) are the joint actuator torques and the forces and moments acting at the spacecraft center of mass. The time optimal algorithm requires that the constraints due to the limits of the the manipulator's actuators and the spacecraft attitude control jets must be stated for the $\mathbf{T}$ vector as a function of the state of the system. It is therefore necessary to transform the dynamic equations into a form where the generalized force vector, called $\mathbf{T}^*$, consists of both the reaction jet forces (F_1 through F_6) and the manipulator actuator torques (T_7, T_8, and T_9), since the saturation constraints are imposed on these forces and torques. The numbering and locations of the reaction jet forces are shown in Figure 2.

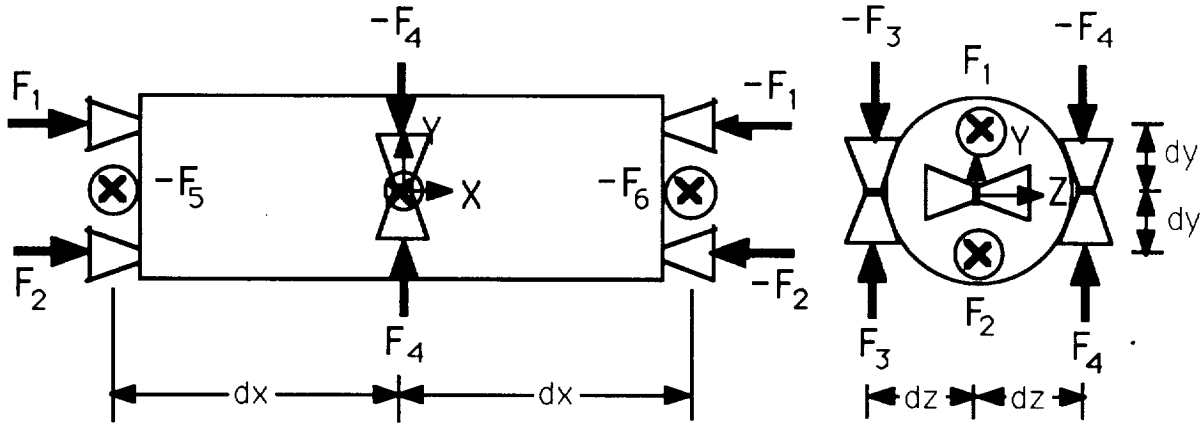

Figure 2. Reaction Jet System

From fundamental mechanics the following transformation may be written:

$$\underline{T}^* = \begin{bmatrix} 1/2 & 0 & 0 & 0 & -1/(2dy) & 0 & 0 & 0 & 0 \\ 1/2 & 0 & 0 & 0 & 1/(2dy) & 0 & 0 & 0 & 0 \\ 0 & 1/2 & 0 & 0 & 0 & 1/(2dz) & 0 & 0 & 0 \\ 0 & 1/2 & 0 & 0 & 0 & -1/(2dz) & 0 & 0 & 0 \\ 0 & 0 & 1/2 & 1/(2dx) & 0 & 0 & 0 & 0 & 0 \\ 0 & 0 & 1/2 & -1/(2dx) & 0 & 0 & 0 & 0 & 0 \\ 0 & 0 & 0 & 0 & 0 & 0 & 1 & 0 & 0 \\ 0 & 0 & 0 & 0 & 0 & 0 & 0 & 1 & 0 \\ 0 & 0 & 0 & 0 & 0 & 0 & 0 & 0 & 1 \end{bmatrix} \underline{T} \tag{6}$$

Using Equation (6), Equation (5) is then transformed into the form:

$$\underline{m}^*(\Phi)\,\ddot{S} + \underline{b}^*(\Phi)\,\dot{S}^2 = \underline{T}^* \tag{7}$$

In this form, the limits on both the capabilities of the reaction jets' forces and the joint motors' torques may easily be taken into account in the formulation of the Limit Curve. The limits on these torques and forces may be expressed as any function of the state of the system:

$$T^*_{imin}(\Phi, \dot{\Phi}) \le T^*_i \le T^*_{imax}(\Phi, \dot{\Phi}) \tag{8}$$

The Limit Curve is found by noting that for each generalized force, a path acceleration value can be calculated as a function of the path position and velocity from Equation (8), or:

$$\ddot{S} = \frac{T^*_i - b^*_i \dot{S}^2}{m^*_i} \tag{9}$$

Note that b^*_i and m^*_i are elements of the vectors $\underline{m}^*$ and $\underline{b}^*$ respectively. From Equation (9), and the limits on forces and torques, it is possible to calculate the range of path accelerations permitted by each joint actuator and reaction jet. The range of accelerations allowed by the complete system is then defined by the limits:

$$\ddot{S}_{min} = \max_i \left(\frac{T^*_{imin} - b^*_i \dot{S}^2}{m^*_i} \right)$$

(10)

$$\ddot{S}_{max} = \min_i \left(\frac{T^*_{imax} - b^*_i \dot{S}^2}{m^*_i} \right)$$

The maximum velocity allowed by the system at any point along the path, $\dot{S}_m$ (S), occurs when the range of allowable $\ddot{S}$ decreases to zero, or $\ddot{S}_{max} = \ddot{S}_{min}$. The function $\dot{S}_m(S)$ plotted in the phase plane defines the Limit Curve which is used by the algorithm to find the optimal switching

points as described in detail in reference [5]. Any conventionally planned trajectory lying above the optimal trajectory in the phase plane will violate the constraints imposed by the joint motors and the reaction jets.

This technique has been implemented in a computer software package with extensive computer graphics to aid the planner in visualizing the results of the optimization.

5. Examples

This section describes the application of the planning technique to the example system shown in Figure 1, whose parameters are given in Table I. The system's masses were chosen so that the manipulator's motions would produce significant disturbances on the spacecraft.

Table I. Space Manipulator Parameters.

	Spacecraft	Link 1	Link 2
Mass	80. kg	4. kg	4. kg
Length	3. m	1. m	1. m
Diameter	1. m	0.5 m	0.5 m
Principle Moments of Inertia:			
about X	20. kg-m^2	0.01 kg-m^2	0.01 kg-m^2
about Y	70. kg-m^2	0.34 kg-m^2	0.34 kg-m^2
about Z	70. kg-m^2	0.34kg-m^2	0.34 kg-m
Maximum Joint Motor Output:		15 N-m	
Maximum Reaction Jet Output:		10 N	
Reaction Jet Locations:	dx = 1.25 m	dy = 0.4 m	dz = 0.4 m

The manipulator path for the case discussed is shown in Figure 3. The Limit Curve and optimal trajectory for this case are shown in Figure 4, along with a conventionally planned trajectory. The optimal trajectory required to complete this maneuver is 3.739 seconds, a significant improvement compared to approximately 5.4 seconds required by the conventional plan which uses constant velocity and accelerations. Figure 5 shows that for the optimal trajectory none of the manipulator joint actuators are used to their full capacity; the maximum torque capabilities are shown as hash marks on the vertical axes of each plot. Hence the manipulator's speed is governed by the capabilities of the reaction jets which are at their bounds during the motion, as may be seen in Figure 6. These suggest that this manipulator might be designed with smaller and less powerful motors, which would both reduce system weight and improve performance.

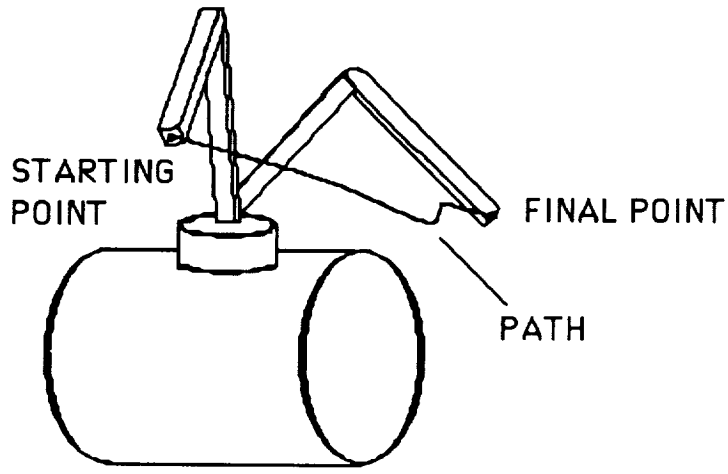

Figure 3. A Three Dimensional View of a Manipulator Path.

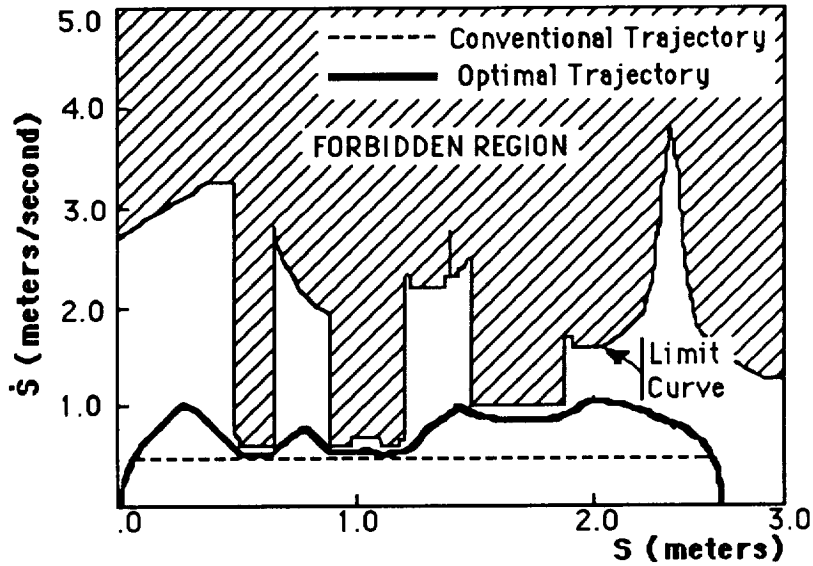

Figure 4. Limit Curve, Optimal and Conventional Trajectories for Example System and Path.

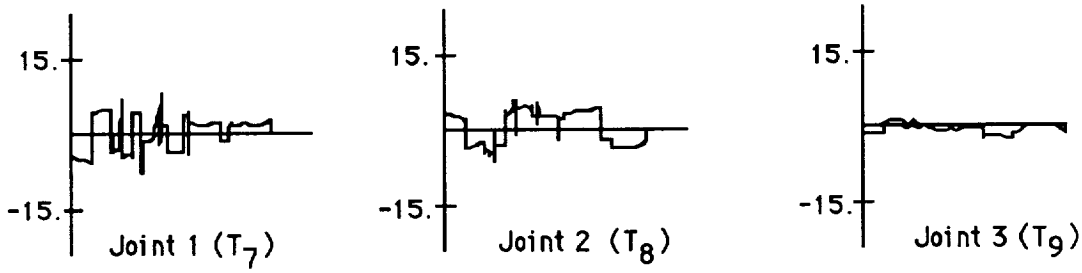

Figure 5. Manipulator joint motor torque profiles (N-m) as a function of Path Distance, S (m).

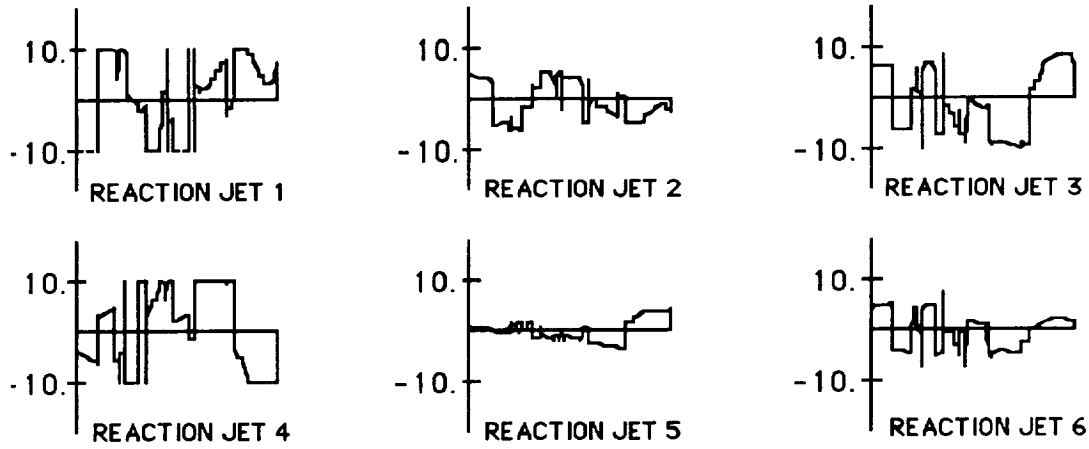

Figure 6. Reaction Jet Force Profiles (N) as a function of Path Distance, S (m).

An independent dynamic simulation was used to verify the results obtained by the algorithm [11]. It showed that the manipulator followed its prescribed path and the spacecraft remained virtually stationary when the joint torques and reaction jet forces calculated with the algorithm were used as dynamic feedforward signals to drive a full nonlinear model of the system: only very small errors were observed due to slight differences between the models and the integration techniques used by the two programs. For example, the simulation showed linear spacecraft displacements of

the less than .0006 meters. In real systems modelling errors can lead to undesired spacecraft motions, even with dynamic feedforward. These can easily be corrected by the spacecraft's attitude control system. Figure 7 shows simulation results for the case where the properties of the system used in the planning algorithm were in error by a few percent and a relatively simple PD attitude control system was used to compensate for the errors. The figure shows the feedforward reaction forces and the small contribution required from the closedloop controller to reduce the motions of the spacecraft essentially to zero.

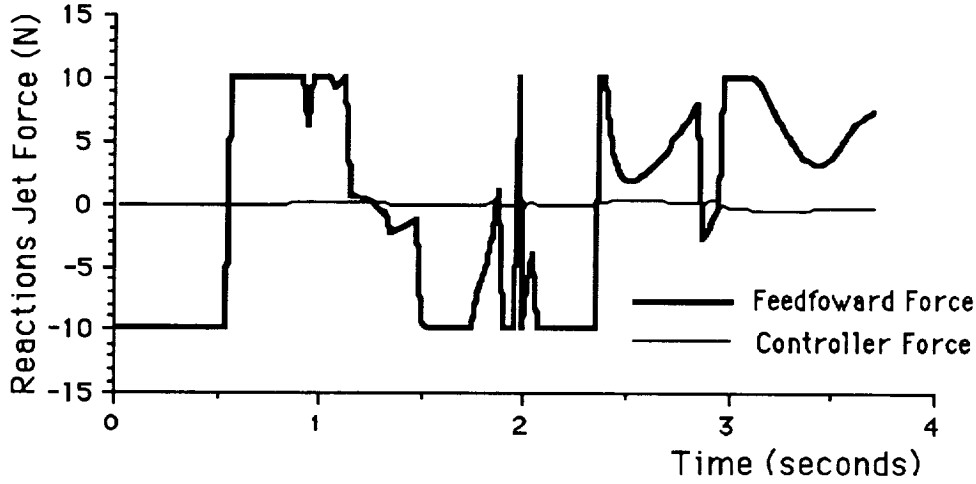

Figure 7. Reaction Jet Forces - Openloop and Control components for System with Modelling Errors.

The importance of the reaction jet forces in holding the spacecraft stationary during the manipulator's motion can be seen in Figures 8a and 8b, which are simulation results for the case where the feedforward signals to the reaction jets are set to zero. Such large linear and angular displacements would be unacceptable in most missions. In most systems the spacecraft's closedloop attitude control system would reduce these disturbance-induced displacements to some degree. However, the simulation results obtained in this study show that trying to control manipulator-disturbed spacecraft motions with feedback control alone can lead to substantial errors, particularly when the attitude control system's bandwidth is limited by system structural resonances and controller sampling times. Based on these results one can conclude that for many systems manipulator disturbances are sufficiently large to require dynamic feedforward compensation in addition to closedloop attitude control.

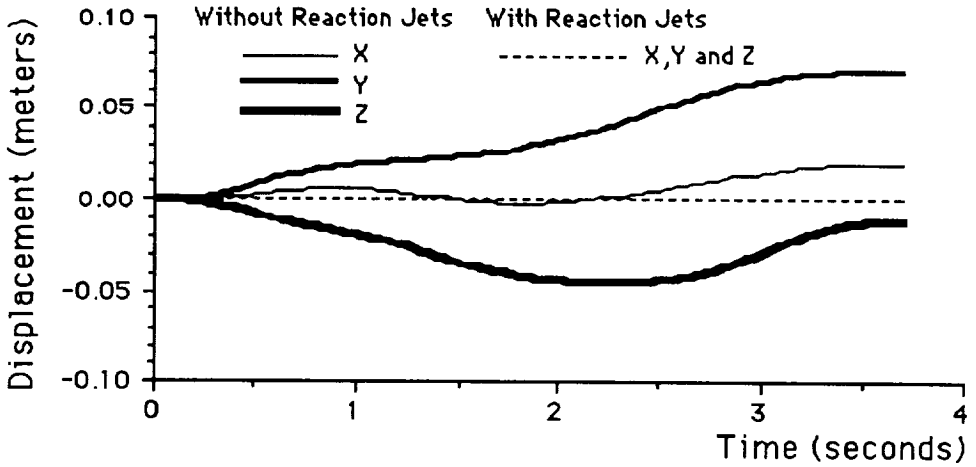

Figure 8 a. Spacecraft Linear Displacements With and Without Reaction Jet Forces (Openloop).

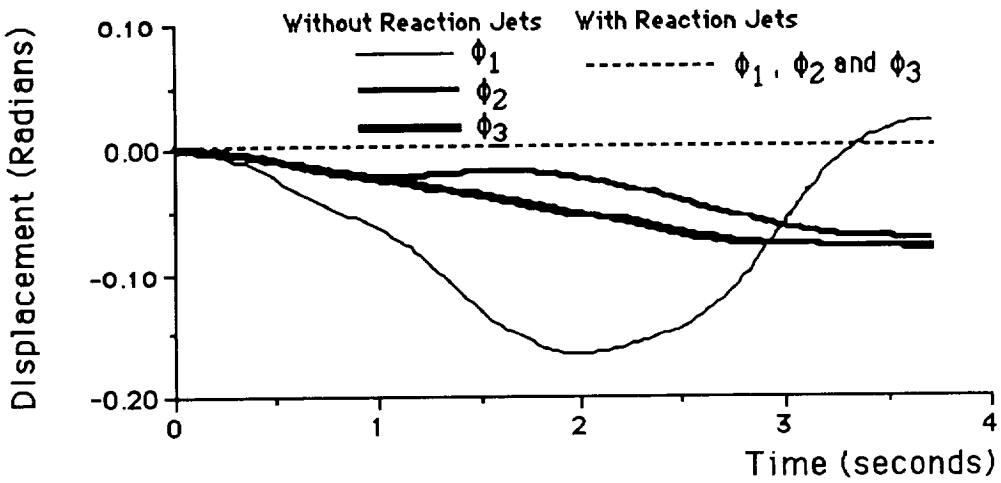

Figure 8 b. Spacecraft Rotations With and Without Reaction Jet Forces (Openloop).

The simulation results obtained in the study also clearly show that saturation of the reaction jet system should be avoided, whether or not manipulator motions are planned in a time optimal manner. Figure 9 shows that the linear motions of the spacecraft became relatively large when the reaction jet forces required to hold the spacecraft during the manipulator's motions exceeded the reaction jet capabilities by 20 percent. The rotational motions also became large. This clearly points out the need to consider the saturation limits of the spacecraft's attitude control system when planning the motions of its manipulator.

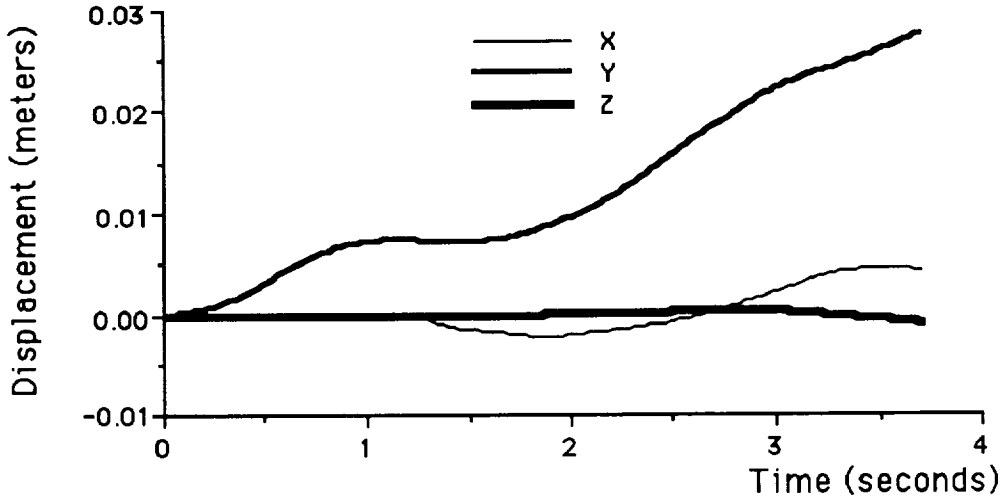

Figure 9. Linear Spacecraft Displacement for System With Reaction Jet Saturation.

6. Conclusions

This paper presents a method for planning the time optimal motions of space manipulators. It considers the constraints of the forces and moments acting on the spacecraft, as well as the constraints of the manipulator joint motors, to calculate a minimum time velocity trajectory for the manipulator. The algorithm has been verified by an independent simulation. The results obtained in the study show that the saturation of a space manipulator system's attitude control jets can be an important problem which should be considered in planning the motions of the manipulator. The technique developed in this paper, combined with a simple attitude control system to compensate for

modelling errors, maybe an effective technique for dealing with this problem. The results obtained in this study also suggest that dynamic feedforward techniques may be an important part of any space manipulator control system.

7. Acknowledgement

This work was supported by NASA Langley Research Center Automation Branch.

8. References

[1] Hollars, M.G., Cannon, R.H., and Alexander, H.L. "Experiments in Advanced Control Concepts for Space Robotics" Tenth Annual AAS Guidance and Control Conference, Keystone, CO, January-February 1987.

[2] Dubowsky, S. and Vafa, Z., "A Virtual Manipulator Model for Space Robotic Systems," Proceedings of NASA Workshop on Space Telerobotics, Jet Propulsion Laboratory, Pasadena,

[3] Vafa, Z. and Dubowsky, S.,"Minimization of Spacecraft Disturbances in Space Robotic Systems," Eleventh Annual AAS Guidance and Control Conference, Keystone, CO, January-

[4] Kahn, M.E. and Roth, B., "The Near-Minimum-Time Control of Open-Loop Articulated Kinematic Chains," Journal of Dynamic System, Measurement and Control, pp 164-172,

[5] Bobrow, J.E., Dubowsky, S., and Gibson, J.S., "Time-Optimal Control of Robotic Manipulators Along Specified Paths," The International Journal of Robotics Research, Vol. 4,

[6] Dubowsky, S., Norris, M.A. and Shiller, Z., "Time Optimal Trajectory Planning for Robotic Manipulators with Obstacle Avoidance: A CAD Approach," Proceedings of the 1986 IEEE Conference on Robotics and Automation, San Francisco, CA, April 1986.

[7] Geering, H., Guzzella, L., Hepner, S.A.R. and Onder, C.H., "Time-Optimal Motions of Robots in Assembly Tasks," IEEE Transactions on Automation Control, pp. 512-518,

[8] Meier, E.B., "An Efficient Algorithm for Bang-Bang Control Systems Applied to a Two-Link Manipulator," PhD Dissertation, Department of Mechanical Engineering, Stanford University,

[9] Shiller, Z. and Dubowsky, S., "Global Time Optimal Motions of Robotic Manipulators in the Presence of Obstacles," IEEE Conference on Robotics and Automation, Philadelphia, PA,

[10] Vance, E.E., "Time Optimal Trajectory Planning for Mobile Manipulators," SM Thesis, M.I.T., Cambridge, MA, 1988.

[11] Torres, M.A., "Dynamic Simulation of Manipulators in Space," Technical Report, Department of Mechanical Engineering, M.I.T., Cambridge, MA, 1987.